

## **ANALYSIS OF PRESSURE AND VELOCITY IN COAL COMBUSTION SYSTEM USING DPM METHOD IN FLUENT SOFTWARE**

**Bharat Bhushan<sup>1</sup>, Ravindra kumar<sup>2</sup>, Shruti Mishra<sup>3</sup>**

<sup>1</sup>Sr.Lecturer in Department of Mechanical Engineering,

<sup>2</sup>Lecturer in Department of Mechanical Engineering,

<sup>3</sup>Lecturer in Department of Computer Engineering,

Gurgaon Institute of Technology, Gurgaon-122413, India

**Abstract:** In this paper computational analysis of pressure and velocity in coal combustion system using the fluent software is analysed. The combustion of coal is used in circulating fluidized bed combustion system. This work is concerned about gas–solid two-phase mixtures flowing upwards through the fast beds. The type of information resulting from various ways of analyzing the pressure variations and the effect of superficial velocity on pressure in fluidized beds are discussed. This paper presents the standard k– $\epsilon$  model and two-phase turbulence model was used to describe the gas–solids flow in a CFB. The analysis of velocity and pressure in coal combustion is done by discrete phase model (DPM) and non pre mixed combustion in species model. The flow velocity and pressure variation in the system were modeled by solving the continuity and momentum equations of the gas flow by using the CFD. The fluidizing velocity has taken (4.5-6) m/s and the effects of operating parameters on pressure, such as gas velocities are discussed. As a result of analysis, the variation in superficial velocity, does affect the pressure in different mean fractions in the combustion zone of the combustor. The results show that if the fluidizing velocity increases then the total and dynamic pressure also increases.

**Keywords:** *Finite volume method, coal, superficial velocity, two-phase flow, discrete phase model, turbulence model, fluidized bed combustion*

### **1. Introduction**

Circulating fluidized bed combustors (CFBCs) are considered in some respects to be an improvement over the traditional methods of coal combustion. Operation of industrial CFBCs has confirmed many advantages including fuel flexibility, broad turn-down ratio, high combustion efficiency, low NO<sub>x</sub> emissions and high sulphur capture efficiency. These characteristics assure increasing commercialization of CFBC in power generation applications. Although CFBC technology is becoming more common, there are some significant uncertainties in predicting performance in large-scale systems. Technical knowledge about design and operation of CFBC is widely available, but little has been done in the field of mathematical modeling and analysis of combustion in CFBCs. Fluidized beds suspend solid fuels on upward-blowing jets of air during the combustion process. The result

is a turbulent mixing of gas and solids. When a fluidized bed is operated above the terminal velocity of the particles, they are carried out of the bed. The fluidization process begins when a bed of inert material (usually sand), which is a solid granular particle, is suspended by a flow of air or gas (air). This flow is injected into the combustion chamber from the bottom and from the side. Combustion systems for solid fuels FBC reduces the amount of sulfur emitted in the form of SO<sub>x</sub> emissions.

### **2. Literature review**

Filip Johnsson worked on [1] the interaction between a fluidized bed and the air-feed system (pipes, valves, and fan and air plenum) was studied in a 8:5×0:7×0:12 m cold circulating fluidized bed unit operated with Group B solids. The study comprises measurements of pressure fluctuations in the bed and in the air plenum as well as of the air flow into the bed. The configuration of the air-feed system was changed by means of valves at two locations in the system. Atsushi Tsutsumi [2] developed on artificial neural networks (ANNs) were proposed to model nonlinear dynamic behaviors of local voidage fluctuations induced by highly turbulent interactions between the gas and solid phases in circulating fluidized beds. The fluctuations of local voidage were measured by using an optical transmittance probe at various axial and radial positions in a circulating fluidized bed with a riser of 0.10 m in inner diameter and 10 m in height. The ANNs trained with experimental time series were applied to make short-term and long-term predictions of dynamic characteristics in the circulating fluidized bed. For the training of ANNs, the error back-propagation algorithm was used with the early stop training approach. The effects of the number of iterations and nodes in input and hidden layers on the training behavior of ANNs have been investigated. Jinsen Gao [3] described on experimental and computational studies on the flow behavior of a gas–solid fluidized bed with disparately sized binary particle mixtures. The mixing/segregation behavior and segregation efficiency of the small and large particles are investigated experimentally. The simulation results are in reasonable agreement with experimental data. The results showed that the smaller particles are found near the bed surface while the larger particles tend to settle down to the bed bottom in turbulent fluidized bed. The calculated results

also show that the small particles move downward in the wall region and upward in the core.

G.N. Ahuja focused on [4] the hydrodynamics of a gas–solid fluidized bed was studied using a combination of experiments and CFD simulations. A multifluid Eulerian model incorporating the kinetic theory for solid particles is used to simulate the gas–solid flow. The effects of superficial gas velocity, presence of draft tube and type of sparging on the solid hold-up and solid circulation patterns have been studied with the help of experiments and CFD simulations. A 2D multifluid Eulerian model integrating the kinetic theory of granular flows is developed. Liang Yu presented on [5] A new numerical model based on the two-fluid model (TFM) including the kinetic theory of granular flow (KTGF) and complicated reactions has been developed to simulate coal gasification in a bubbling fluidized bed gasifier (BFBG). The collision between particles is described by KTGF. The coal gasification rates are determined by combining Arrhenius rate and diffusion rate for heterogeneous reactions or turbulent mixing rate for homogeneous reactions. The flow behaviors of gas and solid phases in the bed and freeboard can be predicted, which are not easy to be measured through the experiments.

J.C.S.C. Bastos focused on [6] Radial solids velocity profiles were computed on seven axial levels in the riser of a high-flux circulating fluidized bed (HFCFB) using a two-phase 3-D computational fluid dynamics model. The computed solids velocities were compared with experimental data on a riser with an internal diameter of 76 mm and a height of 10 m, at a high solids flux of  $300\text{kgm}^{-2}\text{s}^{-1}$  and a superficial velocity of  $8\text{ms}^{-1}$ . Several hundreds of experimental and numerical studies on CFBs have been carried out at low fluxes of less than  $200\text{kgm}^{-2}\text{s}^{-1}$ , whereas only a few limited useful studies have dealt with high solids flux. Adnan Almuttahir [7] focused on A computational fluid dynamics (CFD) model was developed to simulate the hydrodynamics of gas–solid flow in a circulating fluidized bed (CFB) riser at various fluidization conditions using the Eulerian–Granular multiphase model. The model was evaluated comprehensively by comparing its predictions with experimental results reported for a CFB riser operating at various solid mass fluxes and superficial gas velocities. The predicted solid volume fraction and axial particle velocity were in good agreement with the experimental data within the high density fast fluidization regime. However, the model showed some discrepancy in predicting the gas–solid flow behavior in the riser operating in dense suspension up-flow and low density fast fluidization regimes. Afsin Gungor [8] worked on a dynamic two dimensional model is developed considering the hydrodynamic behavior of CFB. In the modeling, the CFB riser is analyzed in two regions: The bottom zone in turbulent fluidization regime is modeled in detail as two-phase flow which is subdivided into a solid-free bubble phase and a solid-laden emulsion phase. In the upper zone core–annulus solids flow structure is established. Simulation model takes into account the axial and radial distribution of voidage, velocity and pressure drop for gas and

solid phase, and solids volume fraction and particle size distribution for solid phase. The model results are compared with and validated against atmospheric cold bed CFB units' experimental data given in the literature for axial and radial distribution of void fraction, solids volume fraction and particle velocity, total pressure drop along the bed height and radial solids flux. Hideya Nakamura [9] presented on modeling of particle fluidization behaviors in a rotating fluidized bed (RFB) was conducted. The proposed numerical model was based on a DEM (Discrete Element Method)-CFD (Computational Fluid Dynamics) coupling model. Fluid motion was calculated two dimensionally by solving the local averaged basic equations. Particle motion was calculated two-dimensionally by the DEM. Calculation of fluid motion by the CFD and particle motions by the DEM were simultaneously conducted in the present model. F. Okasha and M. Miccio [10] focused on a simple mathematical model has been developed to simulate the wet jet in fluidized bed. The different stages involved inside the jet zone have been estimated and analyzed. The evaporation stage of traveling droplets through the jet flare has been treated. The rates of evaporation of each size at all positions along the jet flare have been estimated according to the velocities and surrounding conditions. The final droplet sizes have been determined. Moreover, the total evaporation rate from traveling droplets, before collision either with entrained sand particles or flare boundaries, has been estimated.

### 3. CFB Model Creation and Grid Generation in Gambit

For the furnace as explained in a two dimensional model is created in GAMBIT 2.3.16. The 2D view of the furnace after modeling is as shown in Fig.1

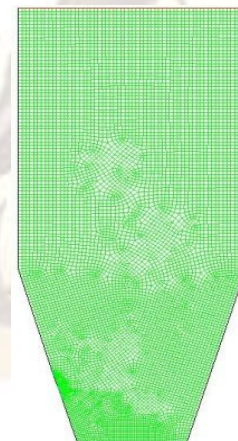


Fig. 1 View of the model in 2D after modeling in GAMBIT 2.3.16

GAMBIT 2.3.16 was used for making 2D furnace geometry with width of 3.2m from the lower part and height 15m. Coarse mesh size of 0.01m was taken in order to have 9365 cells (18952 faces) and 9588 nodes for the whole geometry. It was used in order to have better accuracy. But using mesh results in 9365 cells (18952 faces), which requires smaller time steps, more number of iterations per time step and 4



times more calculation per iteration for the solution to converge.

$$H = \sum_j Y_j H_j \quad (2)$$

#### 4. Selection of models for analysis

FLUENT 6.2.16 was used for analysis. 2D segregated 1st order implicit steady solver is used. (The segregated solver must be used for multiphase calculations). Standard k-ε model with standard wall functions were used.

The model constants are tabulated as:

Table 1 .Model constants used for analysis as given below

Cmu	0.09
C1-Epsilon	1.44
C2-Epsilon	1.92
C3-Epsilon	1.3
TKE Prandtl Number	1
TDR Prandtl Number	1.3
Energy Prandtl Number	0.85

The non premixed combustion model is used for combustion and in DPM (discrete phase model) single type injection system is used for the solid fuel combustion.

#### 5. Boundary Conditions

The boundary conditions are as equally important as the selection of the proper mathematical model. Initially, solid particle velocity was set at in minimum fluidization and gas velocity was assumed to have the same value everywhere in the bed. The temperature of the primary and secondary air was also set to 503k and 473k respectively. At the inlet, all velocities of all phases were specified. At the outlet, the pressure was assumed to be Atmospheric pressure. The gas tangential normal velocities on the wall were set to zero (no slip condition). The following boundary equation was applied for the tangential velocity of Particle on the wall.

Boundary	Condition
Inlet1	Primary(Fluidized) Velocity inlet
Inlet2	Secondary Velocity inlet
Particle flow	Mass flow rate
outlet	Pressure-outlet

#### 6. Governing Equations

When the non-adiabatic non-premixed combustion model is enabled, FLUENT solves the total enthalpy form of the energy equation:

$$\frac{\partial}{\partial t}(\rho H) + \nabla \cdot (\vec{v} H \rho) = \nabla \cdot \left( \frac{k}{c_p} \nabla H \right) + S_h \quad (1)$$

Under the assumption that the Lewis number (Le) = 1, the conduction and species diffusion terms combine to give the first term on the right-hand side of the above equation while the contribution from viscous dissipation appears in the non-conservative form as the second term. The total enthalpy  $H$  is defined as

Where  $Y_j$  is the mass fraction of species  $j$  and

$$H_j = \int_{T_{ref,j}}^T c_{p,j} dT + h_j^0(T_{ref,j}) \quad (3)$$

$h_j^0(T_{ref,j})$  is the formation enthalpy of species  $j$  at the reference temperature  $T_{ref,j}$ .

#### 7. Standard k - ε Model

Another class of turbulence models is the two-equation models. The simplest one is the standard  $k - \epsilon$  model, which is proposed by *Lauder and Spalding*. It is widely used in turbulence simulations because of its general applicability, robustness and economy. The two transport equations for the kinetic energy and dissipation rate are solved to form a characteristic scale for both turbulent velocity and length. These scales represent the turbulent viscosity.

The modeled transport equations for  $k$  and  $\epsilon$  in the realizable  $k - \epsilon$  model are

$$\frac{\partial}{\partial t}(\rho k) + \frac{\partial}{\partial x_j}(\rho k u_j) = \frac{\partial}{\partial x_j} \left[ \left( \mu + \frac{\mu_t}{\sigma_k} \right) \frac{\partial k}{\partial x_j} \right] + G_k + G_b - \rho \epsilon - Y_M + S_k \quad (4)$$

$$\frac{\partial}{\partial t}(\rho \epsilon) + \frac{\partial}{\partial x_j}(\rho \epsilon u_j) = \frac{\partial}{\partial x_j} \left[ \left( \mu + \frac{\mu_t}{\sigma_\epsilon} \right) \frac{\partial \epsilon}{\partial x_j} \right] + \rho C_{1\epsilon} S_\epsilon - \rho C_{2\epsilon} \frac{\epsilon^2}{k + \sqrt{\epsilon v}} + C_{1\epsilon} \frac{\epsilon}{k} C_{3\epsilon} G_b + S_\epsilon \quad (5)$$

$$C_1 = \max \left[ 0.43, \frac{\eta}{\eta + 5} \right], \eta = S \frac{k}{\epsilon}, S = \sqrt{2 S_{ij} S_{ij}} \quad (6)$$

In these equations,  $G_k$  represents the generation of turbulence kinetic energy due to the mean velocity gradients.  $G_b$  is the generation of turbulence kinetic energy due to buoyancy.  $Y_M$  represents the contribution of the fluctuating dilatation in compressible turbulence to the overall dissipation rate.  $C_2$  and  $C_{1\epsilon}$  are constants.  $\sigma_k$  and  $\sigma_\epsilon$  are the turbulent Prandtl numbers for  $k$  and  $\epsilon$ , respectively.  $S_k$  and  $S_\epsilon$  are user-defined source terms.

#### 8. Results and discussion

In this paper, the work has been done in fluent software. The pressure and velocity is analysed of coal combustion process in circulating fluidized bed combustor. Fluidizing velocities of 4.5m/s and 6m/s respectively are given to the air as two inlet velocity conditions for the coal combustion process. After that static pressure and velocity magnitude have been performed at these velocity conditions and some of the results obtained are shown below.

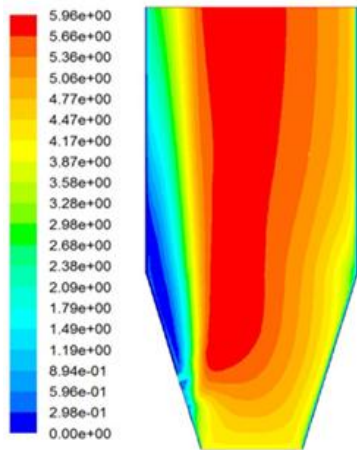


Fig.2 contours of velocity magnitude at 4.5m/s

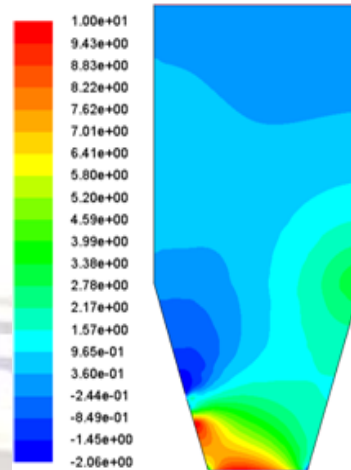


Fig.5 contours of static pressure at 6m/s

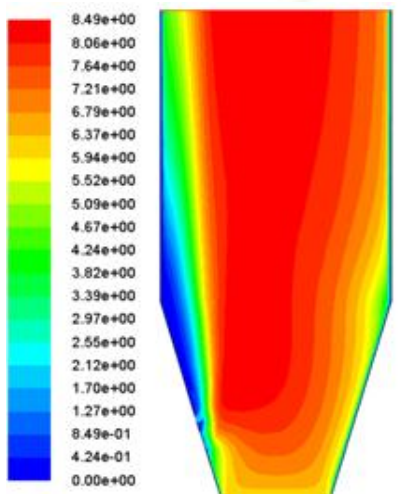


Fig.3 contours of velocity magnitude at 6m/s

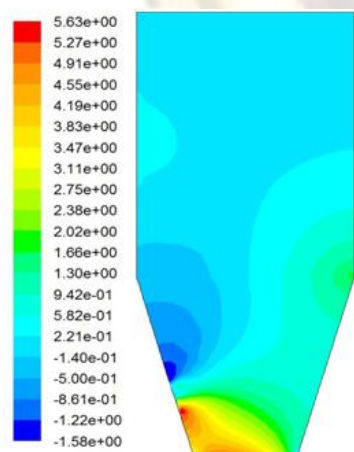


Fig.4 contours of static pressure at 4.5m/s

The value of static pressure is found in the combustor is 5.63 (Pascal) and 10.0 at fluidizing velocity 4.5m/s and 6m/s after combustion process. The static pressure is rapidly increased when air fuel velocity enters in the combustion chamber. In the combustor, maximum static pressure is at the inlet points of the furnace.

The total velocity is found in the CFB combustor is 5.96m/s and 8.49m/s after combustion process at fluidizing velocity 4.5m/s and 6m/s respectively. Fig.1 and 2 show the maximum velocity profile in the middle zone of the combustor during the combustion including primary and secondary air.

*8.1 Behaviour of velocity magnitude at different Mass flow rates of fuel*

Following plot of mass fraction of velocity magnitude vs. mass flow rate of fuel (kg/s) is obtained at different mass flow rate of fuel particles, which shows that velocity increases when the mass flow rate is increased. This is because of the effect of primary and secondary air.

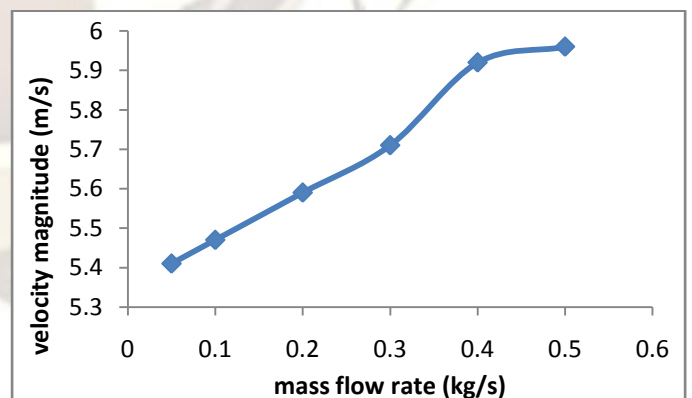


Fig.6 Velocity magnitude vs. mass flow rate of fuel (kg/s)

*8.2 Behaviour of Pressure at different fluidizing velocities*

Following plots of various pressures vs. inlet air velocity obtained at different fluidizing pressures. This plots show that pressure increases as air velocity is increased. This is

because with increase in air velocity and mass flow rate of fuel in the combustor increases thereby increasing the pressure across the combustor. In this fig.7, when the fluidizing velocity is 4m/s at the inlet of combustor then the static pressure is observed 5.63 Pascal after coal combustion in the combustor of CFB i.e. the static pressure is increases with increasing the inlet velocity. The same conditions are for total and dynamic pressure.

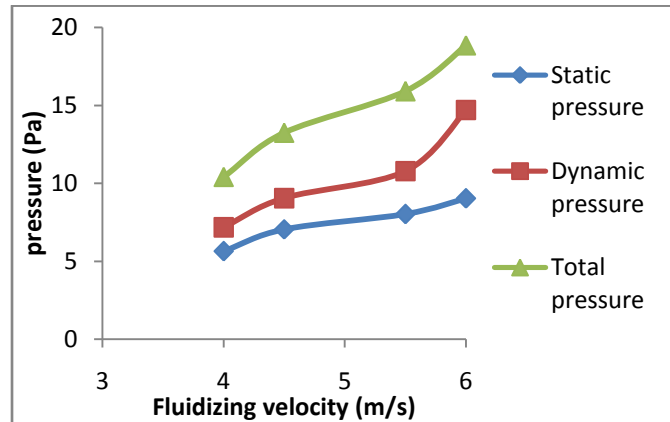


Fig.7 Pressures vs. different fluidizing velocity.

## 9. Conclusions

The following conclusions are drawn:

1. Maximum static pressure increases from 5.63Pa to 10Pa, when fluidizing velocity is increased from 4.5m/s to 6m/s. This increase in the static pressure inside the combustion chamber is because there is no leakage of air from the combustion chamber.
2. Maximum velocity magnitude inside the chamber is due to resultant velocity of primary and secondary air which is flowing into the chamber through two inlets. At a primary velocity of 4.5m/s of air the maximum velocity magnitude is 5.96 m/s. As primary velocity increases to 6m/s, the maximum velocity magnitude also increases to 5.96 m/s and 8.49 m/s.
3. Maximum total pressure increases from 10.4 Pa to 22 Pa, when fluidizing velocity is increased from 4.5m/s to 6m/s. Maximum total pressure values are more than maximum static pressure values at the same fluidizing velocity as it includes dynamic pressure also.

## Notation

$\rho$  = Density  
 $\vec{V}$  = Velocity vector  
 $p$  = Static pressure  
 $\vec{\tau}$  = Stress tensor  
 $\rho\vec{g}$  = Gravitational body force  
 $P$  = Pressure  
 $\mu_{eff}$  = Effective viscosity

$K$  = Turbulent kinetic energy  
 $\varepsilon$  = Dissipation rate of turbulent kinetic energy  
 $T$  = Temperature  
 $g$  = Acceleration due to gravity  
 $k_{eff}$  = Effective conductivity  
 $k_t$  = Turbulent thermal conductivity  
 $\mu$  = molecular viscosity  
 $I$  = unit tensor  
 $h$  = Sensible enthalpy

## References

- [1] Filip Johnsson, Pressure and flow fluctuations in a fluidized bed—interaction with the air-feed system, Department of Energy Conversion, University of Technology, S-412 96 Goteborg, Sweden.
- [2] Atsushi Tsutsumi, Modeling Nonlinear Dynamics Of Circulating Fluidized Beds Using Neural Networks, Department of Chemical System Engineering, The University of Tokyo, Tokyo 113-8656, Japan.
- [3] Jinsen Gao, Experimental and computational studies on flow behavior of gas–solid fluidized bed with disparately sized binary particles, Particuology 6 (2008) 59–71, China University of Petroleum, Changping, Beijing 102249, China.
- [4] G.N. Ahuja, CFD and experimental studies of solids hold-up distribution and circulation patterns in gas–solid fluidized beds, Institute of Chemical Technology, Matunga, Mumbai 400019, India.
- [5] Liang Yu, Numerical simulation of the bubbling fluidized bed coal gasification by the kinetic theory of granular flow (KTGF), Fuel 86 (2007) 722–734, Institute of Process Engineering, Chinese Academy of Sciences, 100080 Beijing, China.
- [6] J.C.S.C. Bastos, Modelling and simulation of a gas–solids dispersion flow in a high-flux circulating fluidized bed (HFCFB) riser, Catalysis Today 130 (2008) 462–470, State University of Campinas, Campinas, Sao Paulo, Brazil.
- [7] Adnan Almuttahir, Computational fluid dynamics of a circulating fluidized bed under various fluidization conditions, Chemical Engineering Science 63 (2008) 1696 – 1709, University of British Columbia, 2360 East Mall, Vancouver, B.C., Canada V6T 1Z3.
- [8] Afsin Gungor, Hydrodynamic modeling of a circulating fluidized bed, Powder Technology 172 (2007) 1–13, Istanbul Technical University, Mechanical Engineering Faculty, Gumussuyu, 34437, Istanbul, Turkey.
- [9] Hideya Nakamura, Numerical modeling of particle fluidization behavior in a rotating fluidized bed, Powder Technology 171 (2007) 106–117, Department of Chemical Engineering, Osaka Prefecture University, 1-1, Gakuen-cho, Sakai, Osaka 599-8531, Japan.
- [10] F. Okasha and M. Miccio, Modeling of wet jet in fluidized bed, Chemical Engineering Science 61 (2006) 3079 – 3090, Department of Mechanical Engineering, Mansoura University, Mansoura, Egypt.